Mon. Not. R. Astron. Soc. **336,** 1099–1108 (2002)

Optical spectroscopy of X-Mega targets – IV. CPD −59°2636: a new O-type multiple system in the Carina Nebula

J. F. Albacete Colombo,[1⋆†‡] N. I. Morrell,[1⋆§¶] G. Rauw,[2] M. F. Corcoran,[3,4‖] V. S. Niemela[1†⋆⋆] and H. Sana[2††]

[1] *Facultad de Ciencias Astronómicas y Geofísicas, Universidad Nacional de La Plata Paseo del Bosque S/N, 1900 La Plata, Argentina*
[2] *Institut d'Astrophysique, Université de Liège, Allée du 6, Août, Bât B5c, B-4000 Liège, (Sart Tilman), Belgium*
[3] *Universities Space Research Association, 7501 Forbes Blvd, Ste 206, Seabrook, MD 20771, USA*
[4] *Laboratory for High Energy Astrophysics, Goddard Space Flight Centre, Greenbelt, MD 20771, USA*

Accepted 2002 June 7. Received 2002 June 3; in original form 2002 April 23

ABSTRACT

High-resolution optical spectroscopy of CPD −59°2636, one of the O-type stars in the open cluster Trumpler 16 in the Carina Nebula, reveals this object to be a multiple system displaying triple lines which we label as components A, B and C of spectral types O7 V, O8 V and O9 V, respectively. From our radial velocity measurements we find that the components A and B form a close binary with a period of 3.6284 d, and we obtain the first circular radial velocity orbit for this system with semi-amplitudes of 184 and 192 km s^{-1}, leading to minimum masses of 10.1 and 9.7 $M_{\odot}$. We find that the component C is a single lined binary with a period of 5.034 d and semi-amplitude of 48 km s^{-1}. We also analyse the X-ray radiation from CPD −59°2636, finding neither appreciable overluminosity nor phase-related X-ray flux variations.

Key words: binaries: general – stars: early-type – stars: fundamental parameters – stars: individual: CPD −59°2636 – open clusters and associations: individual: Trumpler 16 – X-rays: stars.

1 INTRODUCTION

The spectroscopic study of early-type stars in young open clusters is one of the most straightforward ways to detect massive binary stars. The Carina Nebula (NGC 3372), with its rich population of O-type stars, is one of the best places in our Galaxy for the study of massive stars. CPD −59°2636 ($V = 9.31$, $\alpha_{2000} = 10^{\rm h}45'13''$, $\delta_{2000} = -59°44'20''$; Massey & Johonson 1993), or Trumpler 16-110 (Feinstein, Marraco & Muzzio 1973), is a probable member of Trumpler 16, one of the young open clusters located in the Carina region.

Spectral classifications between O7 V and O8 V have been determined for CPD −59°2636 by different authors. The most recent is O8 V, assigned by Massey & Johonson (1993). Moreover, Levato et al. (1991) found that this star exhibits radial velocity variations with a peak amplitude of about 60 km s^{-1}, indicating that CPD −59°2636 is probably a multiple system. Such systems provide valuable astrophysical laboratories for the direct determination of fundamental parameters of the stars, whose knowledge is crucial to test evolutionary models.

In fig. 1 of the first paper of this series (Albacete Colombo et al. 2001) CPD −59°2636 is the star located 26 arcsec north of CPD −59°2635, and it is also detected as a relatively bright X-ray source on the corresponding *ROSAT* High Resolution Imager (HRI) image.

We have observed CPD −59°2636 in the context of the X-Mega international campaign (Corcoran et al. 1999) which involves spectroscopic observations of hot stars detected as X-ray sources. According to Chlebowski & Garmany (1991), intense X-ray emission in O-type stars could be explained as a result of wind collisions in binary or multiple systems. Thus we decided to conduct a detailed spectroscopic monitoring of CPD −59°2636 in order to explore the nature of its radial velocity variations.

An inspection of our first high-resolution spectrograms revealed triple lines present in some of them, indicating that CPD −59°2636 was a multiple system. Additional observations confirmed this hypothesis, as will be shown in this paper.

⋆E-mail: albacete@lilen.fcaglp.unlp.edu.ar
† Visiting Astronomer, CASLEO, operated under agreement between CONICET and National Universities of La Plata, Córdoba and San Juan, Argentina.
‡ Fellow of CIC, Prov. de Buenos Aires, Argentina.
§ Visiting Astronomer, CTIO, NOAO, operated by AURA Inc., for NSF.
¶ Member of Carrera del Investigador Científico, CONICET, Argentina.
‖ Present address: Universities Space Research Association/Laboratory for High Energies Astrophysics, GSFC, Greenbelt, MD 20771, USA.
⋆⋆ Member of Carrera del Investigador Científico, CIC, Prov. de Buenos Aires, Argentina.
†† Research Fellow FNRS, Belgium.

Table 1. Instrumental configuration for different observing runs.

Run Id.	Date	Observatory	Telescope [m]	Spectrograph	Detector	$\lambda/\Delta(\lambda)$	Spec. range [Å]	No. obs.
1	March 1997	CASLEO	2.15	REOSC	Tek 1024	15000	3500–6000	1
2	March 1997	ESO	1.5	B&C	ESO CCD*39	3000	3850–4800	6
3	January–February 1998	CASLEO	2.15	REOSC	Tek 1024	15000	3500–6000	5
4	January–February 1999	CASLEO	2.15	REOSC	Tek 1024	15000	3500–6000	5
5	April–May 1999	ESO	1.5	FEROS	EEV CCD	48000	3650–9200	5
6	March 2000	CASLEO	2.15	REOSC	Tek 1024	15000	3500–6000	5
7	May 2000	ESO	1.5	FEROS	EEV CCD	48000	3650–9200	3
8	February–March 2001	CASLEO	2.15	REOSC	Tek 1024	15000	3500–6000	4

2 OBSERVATIONS

The observations on which this study is based have been obtained at two different southern observatories.

20 echelle CCD and two Cassegrain spectra of CPD −59°2636 were obtained at the Complejo Astronómico El Leoncito (CASLEO), San Juan, Argentina, between 1997 and 2001 with the 2.15-m Jorge Sahade Telescope. The spectrographs used were the REOSC-échelle Cassegrain spectrograph[1] and the Boller and Chivens (B&C) Cassegrain spectrograph, respectively.

14 spectra of CPD −59°2636 were obtained at the European Southern Observatory (ESO) 1.5-m telescope. The spectrograph used were the B&C Cassegrain spectrograph and the Fiber-fed Extended Range Optical Spectrograph (FEROS, Kaufer et al. 1999).

Table 1 gives details about the instrument configuration used in each observing run.

Part of the data obtained with the B&C spectrograph at ESO 1.5-m telescope are affected by a strange fringing pattern (Turatto, Tighe & Castillo 1997), which affects the wavelength range 4050–4250 Å in the used instrument configuration. Given the variability of the fringing pattern, and in order to avoid amplification of the fringes in the stellar spectra, the data were not flat-fielded.

The observations obtained at CASLEO were processed and analysed with IRAF[2] routines at La Plata Observatory.

The data obtained at ESO were reduced using the MIDAS software developed at ESO.

3 SPECTRAL CLASSIFICATION

CPD −59°2636 has been classified as O8 V by Walborn (1982a) and Massey & Johonson (1993), and as O7 V by Levato & Malaroda (1982).

A preliminary inspection of our high-resolution spectra revealed that CPD −59°2636 is a multiple system, with three sets of absorption lines present in its spectrum, all of which belong to late O-types, which we labelled as components A, B and C. Some differences in linewidths and intensities helped in identifying each component in our observations. The component C has lines that are narrower than the other two components, and it was the first to be identified on every spectrogram. To distinguish between components A and B was more difficult and we had to wait until the period of this close pair was determined to properly identify each component on our spectra (see Section 4.1 for details).

[1] Originally built by REOSC and Liège Observatory, and on long term loan to CASLEO.

[2] Image Reduction and Analysis Facility, distributed by NOAO, operated by AURA, Inc. under agreement with NSF.

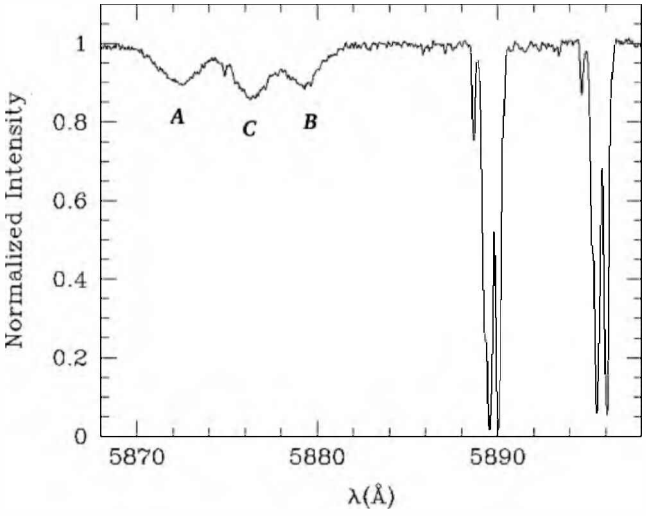

Figure 1. The region containing the He I 5876 Å absorption line in a FEROS spectrum of CPD −59°2636, observed on HJD 2451670.609. Note the complex structure of the interstellar Na I lines.

In Fig. 1 we present one of the FEROS spectra of CPD −59°2636 in the wavelength region containing the He I 5875 Å absorption line, which clearly shows the three stellar components. Also shown in Fig. 1 are the interstellar Na I lines displaying a complex structure due to multiple components along the line-of-sight, already noticed by Walborn (1982b) in the Ca II lines.

With the aim of deriving individual spectral types for each component of CPD −59°2636, we used the spectral classification criteria described by Walborn & Fitzpatrick (1990) in the analysis of our high- and intermediate-resolution spectra. In addition we applied the classification schemes proposed by Conti (1973) and Kerton, Ballantyne & Martin (1999) to the equivalent widths (EW) of He I and He II absorptions. We obtained those EW as averages of several measurements performed on our high-resolution spectra. In order to reduce the effects of the sometimes serious blending of the measured lines (which is evident in Figs 2 and 3), three independent Gaussians were fitted to the observed profiles, using the IRAF NGAUSSFIT task.

Following Conti (1973), we derived the value

$$R = \log(EW_{\mathrm{He\,I}4471}/EW_{\mathrm{He\,II}4542})$$

for each component of CPD −59°2636, finding $R_{\mathrm{A}} = -0.01 \pm 0.21$, $R_{\mathrm{B}} = 0.18 \pm 0.23$, and $R_{\mathrm{C}} = 0.14 \pm 0.18$, corresponding to spectral types O7 V, O8 V and O8 V, respectively.

We also applied the classification scheme proposed by Kerton et al. (1999), considering

$$R = \log(EW_{\mathrm{He\,I}4921}/EW_{\mathrm{He\,II}5411})$$

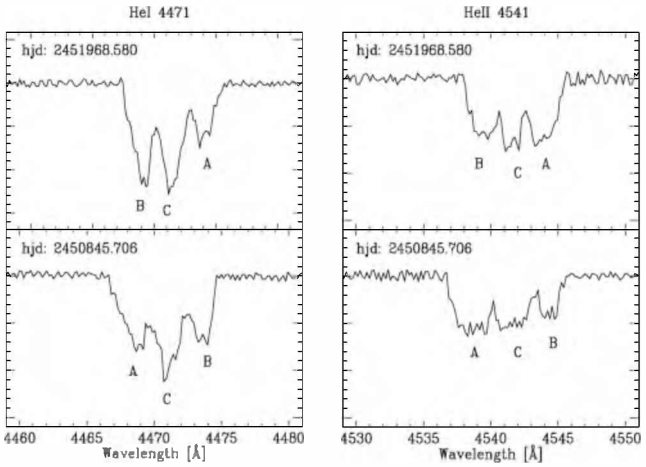

Figure 2. He I 4471 Å and He II 4542 Å absorption lines in two observations of CPD −59°2636. Note the changes in the relative intensity of He I 4471 for component B, which could be affecting the spectral type determination.

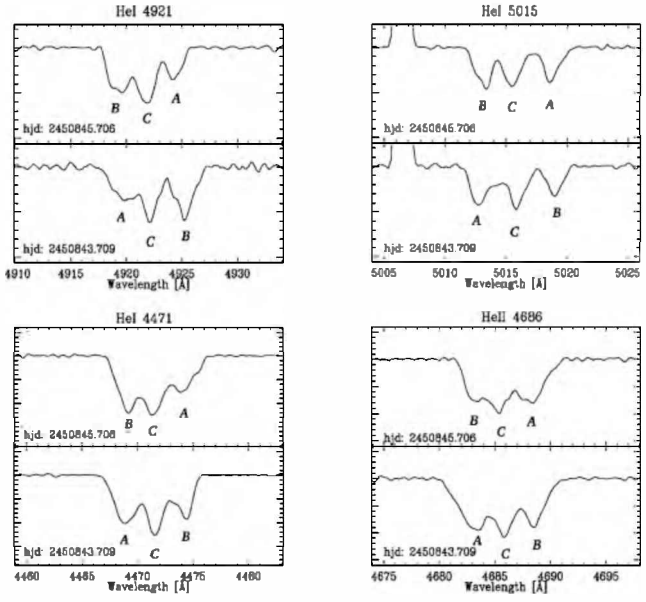

Figure 3. Behaviour of the He I 4471-Å line in different observing dates, in comparison with He I 4921-Å, 5015-Å and He II 4686-Å lines. Only 4471 Å shows clear intensity variations, becoming stronger when the line is blue-shifted, a behaviour identified as the S-S effect.

and we found logarithmic equivalent width ratios $R_A = -0.08 \pm 0.03$, $R_B = -0.07 \pm 0.03$, and $R_C = 0.14 \pm 0.03$, corresponding to the spectral types O8, O8 and O9, for components A, B and C, respectively.

In order to estimate the luminosity class of the component C, we used the criterion proposed by Mathys (1988):

$$\log W^+ = \log EW_{\mathrm{He\,I}4388} + \log EW_{\mathrm{He\,II}4686}\,.$$

The measured EWs were corrected for continuum overlapping of the other two components, estimating this contribution through comparison with equivalent width measurements of single stars of the same spectral types from Mathys (1988). We obtained $\log W_C^+ = 5.47 \pm 0.12 > 5.35$, thus corresponding to luminosity class V.

To get another estimation of the luminosity class of the components A and B, we also used the expression given by Conti & Alschuler (1971):

$$\log W = \log EW_{\mathrm{Si\,IV}4089} - \log EW_{\mathrm{He\,I}4144}$$

finding $\log W_A = -0.13$, and $\log W_B = 0.06$ smaller than $+0.10$ and larger than -0.20, thus indicating that components A and B also belong to luminosity class V.

We then conclude that the three spectral components of CPD −59°2636 are of luminosity class V, as already suggested by the visual inspection of our data, where we noticed, for example, that He II 4686 Å presents strong absorption profiles in agreement with an early evolutionary stage for the stars in this multiple system.

We found that the equivalent widths of some absorption lines of component B (secondary), which we will show forms a close binary system with the component A (primary), are not constant, but display phase-related variations. Such variations are present in He I 4471 Å and probably also in He I 4921 Å and 5015 Å. This behaviour, called 'Struve–Sahade' effect (S-S effect), has been observed in massive close binary systems, and is described by Bagnuolo et al. (1999), as 'the apparent strengthening of the secondary spectrum of a hot binary when the secondary is approaching and the corresponding weakening of the lines when it is receding'. There are a variety of mechanisms that can result in line-intensity variations of binary components as a function of the orbital phase. Wind blanketing and/or heating, obscuration and re-radiation by gas streams could explain the asymmetrical change in the secondary spectrum. Also, Gayley (2001) has suggested that the S-S effect might be due to surface flows generated by irradiation of the stellar surface by the companion.

Fig. 3 shows the profiles of He I 4471, He I 4921, 5015 Å and He II 4686 Å lines at two different observing dates. He I 4471 Å presents intensity variations that could affect the spectral types assigned for components B and (probably) A. Such variations are not clear in the other spectral lines represented in the figure.

Considering the results of the different classification methods and especially relying on the visual inspection of the spectra in order to decide between slightly different results, we arrive to the conclusion that CPD −59°2636 presents at least three stellar components that we labelled as A, B and C, and classify as O7 V, O8 V and O9 V, respectively. Spectral line variations identified as S-S effect can modify the spectral classification of component B, but by less than one subclass, according to our estimations.

4 RADIAL VELOCITY ANALYSIS

From our high-resolution spectrograms of CPD −59°2636, we measured radial velocities fitting three different Gaussians whenever the separation between components was enough to do so. When this was not the case, we used an independent Gaussian fit with fixed parameters in an attempt to deblend the lines.

Our radial velocity determinations show that CPD −59°2636 is a multiple system consisting of a close pair formed by components A and B, and another (single-lined) binary represented by component C which has an orbital period somewhat longer and presents radial velocity variations of smaller amplitude.

For the radial velocity analysis, we used He I and He II spectral lines which are always present in the spectrum of each component, He I 4471, 4922, 5015, 5875 Å and He II 4686 Å. Other He II lines, such as λ 4200, 4542, and 5411 Å show broad profiles, presumably as a consequence of high pressure acting in the line formation region, which must be deeper in the atmosphere than the formation region of the He I lines. As a result, blending effects are more serious in those lines, making less confident the radial velocity determinations derived from them. In addition, He II 4686, lying near the centre of

Table 2. Heliocentric radial velocities for stars A and B of CPD −59°2636, forming a SB2 system. The orbital phases are relative to the time of maximum radial velocity of the component A. All radial velocities, standard deviations (s.d.) and (O-C) are in km s^{-1}. 'Run Id.' is as in Table 1. The standard deviation of the fit is 17 km s^{-1}.

HJD	Phase	A – primary				B – secondary				Run Id.
2 400 000+	ϕ	VR	s.d.	n	O-C	VR	s.d.	n	O-C	
50508.811	0.264	−13	4	4	−12	+26	6	4	+11	1
50534.731	0.407					+155	5	3	+2	2
50535.735	0.684					+140	12	3	+30	2
50536.726	0.957	+176	30	2	−11	−193	15	3	−14	2
50538.707	0.459	−170	21	3	−5	+176	8	3	−13	2
50841.811	0.040	+219	11	5	+19	−186	9	5	+5	3
50843.709	0.563	−142	14	5	+17	+206	7	5	+22	3
50845.706	0.136	+184	12	5	+22	−145	7	5	+6	3
50848.757	0.954	+200	8	5	+13	−155	14	5	+22	3
50850.712	0.493	−138	19	3	+25	+216	18	3	+28	3
51209.741	0.443	−147	8	5	+1	+171	5	5	−1	4
51210.795	0.733	−55	11	5	−11	+48	6	4	−11	4
51216.830	0.396	−106	10	5	+16	+133	18	5	−12	4
51217.637	0.619	−138	14	5	−1	+178	10	5	+18	4
51218.732	0.921	+168	9	5	+4	−147	7	5	+7	4
51300.654	0.499	−161	4	3	+3	+202	5	3	+13	5
51302.559	0.024	+213	5	5	+11	−183	3	5	+11	5
51302.715	0.067	+202	12	5	+11	−172	6	5	+10	5
51304.629	0.594	−140	16	4	+9	+185	4	4	+12	5
51327.620	0.930	+181	2	2	+10	−143	4	2	+18	5
51615.611	0.302	−51	13	5	−11	+58	7	5	−1	6
51617.542	0.834	+65	8	5	−11	−92	13	5	−29	6
51618.636	0.136	+123	23	5	−19	−145	10	5	−13	6
51619.815	0.461	−163	13	5	−7	+173	14	5	−6	6
51620.615	0.681	−83	5	5	+8	+94	9	5	−18	6
51670.609	0.459	−157	6	5	−2	+176	13	5	−3	7
51672.593	0.006	+192	8	5	−10	−200	9	5	−6	7
51968.580	0.581	−171	8	5	−17	+162	8	5	−16	8
51969.576	0.856	+67	6	5	−34	−104	16	5	−15	8
51970.643	0.150	+98	28	5	−30	−132	13	5	−3	8
51971.564	0.404	−158	14	5	−30	+130	20	5	−20	8

an echelle order in CASLEO data, presents higher signal-to-noise ratio than other He II lines.

Our radial velocity determinations are presented in Table 2 for components A and B, and Table 3 for component C, where we list: the heliocentric Julian Date corresponding to each observation, followed by orbital phases computed with the ephemeris of Tables 4 and 5, the corresponding average heliocentric radial velocities, standard deviations, number of lines included in the average, and O-C values, in units of km s^{-1}.

4.1 The orbital periods

We have performed a period search applying to our radial velocity determinations the (Lafler & Kinman 1965, hereafter LK 65) technique, the generalized Fourier analysis (Heck, Manfroid & Mersch 1985 hereafter HMM 85), and the maximum entropy method (Cincotta, Mendez & Nuñez 1995, hereafter CMN 95).

For the pair composed of stars A and B we performed the period search using the absolute radial velocity differences $\|(V_{rA} - V_{rB})\|$, which are better suited for period determinations than individual radial velocities, in cases where the two components have lines so similar that confusion between them is a possible issue. As for the system containing component C, we have only one set of spectral lines, as already mentioned.

We have not found significative differences between the period values obtained from different techniques. Therefore, we adopted a period value of $P_{A+B} = 3.6284 \pm 0.0005$ d for the double-lined close binary system (SB2), and $P_c = 5.034 \pm 0.002$ d for the single-lined binary system (SB1) and used these values in the input for the orbital calculation routines.

If both binary systems are physically related, their systemic velocities will show anti-correlated variations with time. We did not find such variations in our data set. However, the relatively short time baseline covered by our observations (5 yr) might be responsible for those variations not being apparent.

4.2 Orbital solution for the close pair A + B

From our radial velocity measurements we identify components A and B as the primary and secondary, respectively, of the close binary system with period 3.6284 ± 0.0005 d.

We applied a modified version of the code developed by Bertiau & Grobben (1969) in order to obtain the radial velocity orbit of the binary system A + B. The corresponding solution is presented in Table 4 and plotted, along with our radial velocity observations, in Fig. 4. In the orbital solution we assigned weight 0.5 to data from the run labelled as 2, while the other data were given unit weight.

Table 3. Heliocentric radial velocities for component C of CPD −59°2636. The orbital phases are relative to the time of maximum radial velocity in the orbital solution. All radial velocities, s.d. and (O-C) are in km s^{-1}. 'Run Id.' is as in Table 1. The standard deviation of the fit is 11 km s^{-1}.

HJD	Phase	C – component				Run Id.
2 400 000+	ϕ	VR	s.d.	n	O-C	
50 508.811	0.32	−10	3	4	0	1
50 536.726	0.86	+44	22	2	+13	2
50 537.721	0.06	+27	15	2	−15	2
50 538.707	0.26	+12	4	4	+5	2
50 539.720	0.46	−25	9	4	+20	2
50 841.811	0.47	−53	6	5	−6	3
50 843.709	0.84	+29	5	5	+2	3
50 845.706	0.24	+10	6	5	−1	3
50 848.757	0.85	+27	12	5	0	3
50 850.712	0.24	+11	2	5	−1	3
51 209.741	0.55	−58	8	5	−7	4
51 210.795	0.76	+5	14	5	+1	4
51 216.830	0.96	+54	11	5	+10	4
51 217.637	0.12	+38	5	5	+3	4
51 218.732	0.34	−31	8	5	−13	4
51 300.654	0.61	−31	3	6	+11	5
51 301.607	0.80	+10	4	8	−6	5
51 302.559	0.99	+40	4	11	−6	5
51 302.715	0.02	+39	6	9	−5	5
51 304.629	0.40	−22	6	8	+12	5
51 327.620	0.97	+44	3	6	−1	5
51 615.611	0.18	+19	8	5	−6	6
51 617.542	0.56	−54	11	5	−4	6
51 618.636	0.78	+5	7	5	−5	6
51 619.815	0.01	+51	4	5	+6	6
51 620.615	0.17	+40	13	5	+14	6
51 670.609	0.10	+34	3	14	−3	7
51 671.633	0.31	−8	5	12	+1	7
51 672.593	0.50	−41	8	12	+10	7
51 968.580	0.29	−7	10	5	−2	8
51 969.576	0.49	−64	9	5	−14	8
51 970.643	0.70	−14	10	5	+1	8
51 971.564	0.89	+35	6	5	−1	8

The relatively low values found for the minimum masses are indicative of a low inclination of the orbital plane.

4.3 Orbital solution for component C

From the radial velocities listed in Table 3 we computed orbital elements for the single lined binary C using the modified version of the Bertiau & Grobben (1969) code and the period of 5.034 ± 0.002 d determined for this star.

The resulting orbital elements are presented in Table 5. In Fig. 5, we plot the observed radial velocities and the computed orbital solution. Again, we assigned weight 0.5 to the data from run 2 and weight 1.0 to all the remaining data.

As seen in Tables 4 and 5, we obtain for the orbital solution eccentricities that have small, but non-zero, values. In order to check the reliability of these eccentricities, we applied a statistical F-test, following Lucy & Sweeney (1971) finding that the values derived for those parameters are lower than 2.45 times their 1σ error, thus corresponding to a level of significance of only 5 per cent. Consequently, circular orbital fits could also be applied to our data for both binaries, with indistinguishable results.

Table 4. Orbital parameters for the close pair A + B. T_{max} represents the time of maximum radial velocity of the primary component A. The last column gives the error of each parameter.

P (d)	3.6284	$\pm 1 \times 10^{-4}$
e	0.06	±0.03
Ω (°)	355	±15
K_A (km s^{-1})	184	±4
K_B (km s^{-1})	192	±4
γ (km s^{-1})	8	±1
T_{max} (HJD)	2 450 848.94	±0.1
T_{peri} (HJD)	2 450 848.98	±0.1
$a_A \sin i$ ($R_\odot$)	13.2	±0.2
$a_B \sin i$ ($R_\odot$)	13.7	±0.2
$M_A \sin^3 i$ ($M_\odot$)	10.1	±1
$M_B \sin^3 i$ ($M_\odot$)	9.7	±1
$q(M_B/M_A)$	0.96	±0.04

Table 5. Orbital solution for component C. T_{max} represents the time of maximum radial velocity and T_{peri} the time around periastron passage. $F(M)$: mass function for the SB1 binary system. The last column give the error of each parameter.

P (d)	5.034	3×10^{-3}
e	0.09	0.04
Ω (°)	209	30
K_C (km s^{-1})	48	5
γ_{SB1} (km s^{-1})	0	2
T_{max} (HJD)	2 451 217.0	0.5
T_{peri} (HJD)	2 451 215.0	0.5
$a \sin i$ ($R_\odot$)	4.8	0.4
$F(M)$ ($M_\odot$)	0.06	0.02

4.4 The fourth component

Let's now explore the possibility of a fourth component in CPD −59°2636 and its physical nature. In order to rule out the alternative explanation of CPD −59°2636 being a triple system, we have computed the quantity $v_A + (m_B/m_A)v_B$ (proportional to γ_{A+B}) as a function of the 5.034 day period of the SB1 orbital solution of

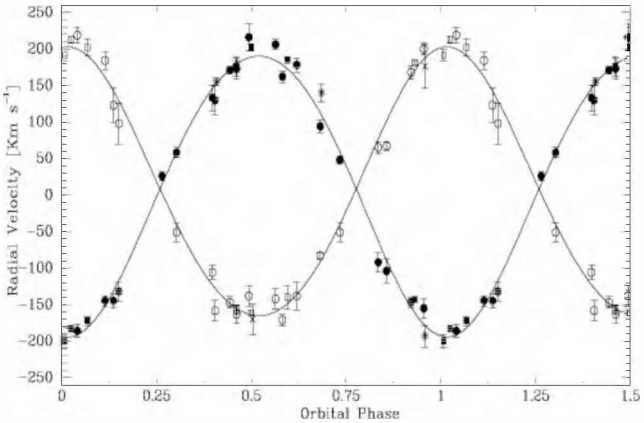

Figure 4. Radial velocity solution for the A + B binary system. The meanings of the symbols are as follows. Open and filled symbols refer to primary A and secondary B components, respectively. Circles represent REOSC-echelle spectra, squares represent FEROS spectra and crosses/asterisks represent B&C spectra.

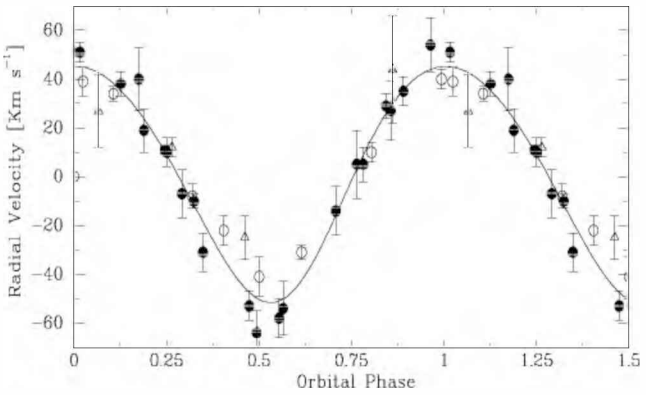

Figure 5. Radial velocity solution for component C. The meanings of the symbols are as follows. Filled circles represent REOSC-echelle spectra, open circles represent FEROS spectra and triangles represent B&C spectra (included in the RV solution with weight = 0.5)

component C. As we see in Fig. 6, there is no clear trend that could indicate that we are dealing with a genuine triple system, because if CPD −59° 2636 were a triple system, the systemic velocity of the pair A + B, i.e. γ_{A+B}, should vary with an amplitude of a bit less than K_C but with the same period of component C (see Table 5).

Another point that argues against a triple system is the stability of such a system. Eggleton & Kiseleva (1995) found that hierarchical systems are stable provided that their configuration is such that $P_{orb}^{out}/P_{orb}^{in} \geqslant X_0^{tott}$ where X_0^{tott} is a function of the mass ratios $q_{in} = m_A/m_B$ and $q_{out} = (m_A + m_B)/m_C$ and the eccentricities of the inner and outer orbits. For values of q_{out} between 1.75 and 3.0 (what we would have for CPD −59° 2636 is ≈2.6), the criterium states that stable orbits will occur if P_{out}/P_{in} is larger than 11. As the observed period ratio (1.39) is much less than the minimum required for dynamical stability, we conclude that CPD −59° 2636 must be a quadruple system.

We can then discuss the possible nature of the fourth star in CPD −59° 2636. It is unlikely that this could be a compact object, because its progenitor would have to be extremely massive and even then, it is not clear whether the age of the system would be sufficient to allow this star to complete its evolution and become a compact object.

From the mass function obtained for this binary (0.06), if we assume for the primary O9 V star a reasonable mass of, say, 18 $M_\odot$, and guess the orbital inclination will be the same as the value estimated for the pair A + B, we find that the companion of star C should be a 4 to 6 $M_\odot$ star, thus an intermediate B-type star.

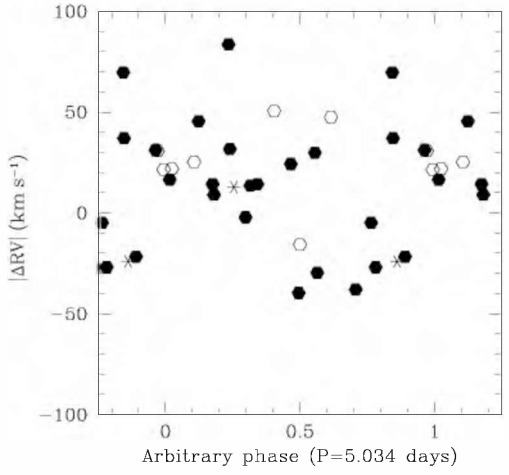

Figure 6. Systemic velocity of SB2 system (γ_{SB2}) as a function of the period of component C (arbitrary phase). The meanings of the symbols are as follows. Stars represent B&C spectra, filled hexagons represent REOSC spectra and open hexagons represent FEROS spectra.

5 PHYSICAL PARAMETERS

In order to estimate the relative contribution of each component of CPD −59° 2636 to the total observed brightness, we have applied the corrected integrated absorption method of Petrie (1940). We measured equivalent widths of He I 4144, 4388, 4471 Å, He II 4541, 4686 Å and Si IV 4089 Å on our high-resolution spectra, and compared them with similar measurements of single stars of the same spectral types obtained by Mathys (1988) and Conti & Alschuler (1971). Those equivalent widths are listed in Table 6.

The derived brightness ratios for each component are as follows: $l_A/L_{TOT} = EW_A/EW_{O7V} = 0.39 \pm 0.05$, $l_B/L_{TOT} = EW_B/EW_{O8V} = 0.30 \pm 0.04$, and $l_C/L_{TOT} = EW_C/EW_{O9V} = 0.26 \pm 0.04$. As the sum of the relative contributions should be equal to 1.0, we normalized our preliminary results, and then we derived individual brightness of $l_A/L_{TOT} = 0.41 \pm 0.05$, $l_B/L_{TOT} = 0.32 \pm 0.04$, and $l_C/L_{TOT} = 0.27 \pm 0.04$.

However, we have to recall that there could be a fourth component in the system, the companion of star C, which has no signature in our spectra.

From the error estimation of the total luminosity of CPD −59° 2636, we derived a maximum value for the luminosity of the fourth component, not presenting any spectral features in our high-resolution spectra. This condition suggests a probably rather faint star contributing about 10 per cent to the total brightness of CPD −59° 2636, which could correspond to a B-type star. This seems to be consistent with our speculation about the mass for the fourth component obtained from the mass function of the SB1 binary.

In order to get individual magnitudes and luminosities for components A, B and C, we adopted for CPD −59° 2636 $V = 9.31$, $E_{B-V} = 0.60$, and $A_v = 1.92$, from Massey & Johonson (1993), hereafter (MJ93). The distance modulus for Trumpler 16 is still a controversial matter, as already discussed, for example, in Rauw et al. (2001), and Benvenuto et al. (2002). As a consequence, we thought that it would be useful to derive the physical parameters for each component, according to two different distance moduli, namely, those obtained by MJ93, $M_V - V_0 = 12.49 \pm 0.09$; and Davidson et al. (2001), $M_V - V_0 = 11.76 \pm 0.18$. Depending on which distance modulus we consider, the absolute visual magnitude of CPD −59° 2636 will be $M_V = -5.10 \pm 0.09$ or $M_V = -4.37 \pm 0.18$, respectively.

In Table 7, we present the derived physical parameters for the CPD −59° 2636 components using the bolometric corrections and effective temperatures from Howarth & Prinja (1989).

The A and B components have been discovered to be a close binary system, and we can estimate new physical parameters for these stars.

As the components of CPD −59° 2636 belong to luminosity class V, we can expect that they fit inside their corresponding Roche lobes. Applying for the radius of the Roche lobe the expression given by Paczynski (1971):

$$\frac{R_{RL}^1}{a} = 0.38 + 0.2 \log\left(\frac{M_1}{M_2}\right) \qquad (1)$$

Table 6. Equivalent widths of absorption lines for single stars and CPD −59° 2636. References labelled with numbers are: (1) Mathys (1988), (2) Conti & Alschuler (1971) and (3) this paper.

Star	S.T.	He I			He II		Si IV	Ref.
		4143 Å	4388 Å	4471 Å	4541 Å	4686 Å	4089 Å	
HD 90273	O7 V	–	0.29	0.60	0.72	0.74	–	1
HD 91824	O7 V	–	0.23	0.55	0.69	0.87	–	1
HD 110360	O7 V	–	0.32	0.74	0.93	0.97	–	1
HD 164492	O7 V	–	0.21	0.63	0.66	0.97	–	1
68 Cyg	O8 V	–	–	0.89	0.64	0.44	0.20	2
HD 41161	O8 V	0.24	–	0.91	0.59	0.79	0.27	2
HD 46056	O8 V	–	–	0.87	0.61	0.83	–	1
HD 73882	O8 V	–	0.33	0.75	0.45	0.77	–	1
HD 5005c	O9 V	0.19	–	0.89	0.43	0.45	0.24	2
HD 46202	O9 V	0.31	–	0.95	0.40	0.55	0.37	2
HD 92504	O9 V	–	0.39	0.91	0.35	0.74	–	1
HD 92555	O9 V	–	0.38	0.95	0.36	0.79	–	1
HD 166546	O9 V	–	0.43	0.85	0.32	0.62	–	1
A	O7 V	0.11 ± 0.02	0.12 ± 0.02	0.20 ± 0.05	0.20 ± 0.05	0.26 ± 0.04	0.05 ± 0.02	3
B	O8 V	0.06 ± 0.02	0.09 ± 0.02	0.20 ± 0.04	0.13 ± 0.04	0.22 ± 0.04	0.06 ± 0.03	3
C	O9 V	0.08 ± 0.02	0.11 ± 0.02	0.18 ± 0.03	0.13 ± 0.03	0.21 ± 0.02	0.04 ± 0.03	3

Table 7. Physical parameters for A + B, and C components in CPD −59° 2636. Effective temperatures and bolometric corrections were taken from Howarth & Prinja (1989). R_{SB} and r_{RL} refer to a Stefan–Boltzmann radii and minimal Roche lobe radii, respectively. V_{syn} refers to the synchronous rotation velocity.

Physical parameters	$M_v - V_0 = 11.76$			$M_v - V_0 = 12.49$		
	A	B	C	A	B	C
M_v	−3.40 ± 0.3	−3.14 ± 0.3	−2.95 ± 0.3	−4.13 ± 0.1	−3.86 ± 0.2	−3.68 ± 0.2
M_{bol}	−7.02 ± 0.3	−6.56 ± 0.3	−6.17 ± 0.3	−7.75 ± 0.1	−7.28 ± 0.2	−6.90 ± 0.2
log(L) ($L_\odot$)	4.71 ± 0.1	4.52 ± 0.11	4.37 ± 0.13	5.00 ± 0.09	4.82 ± 0.08	4.66 ± 0.09
R_{SB} ($R_\odot$)	5.0 ± 0.8	4.9 ± 0.6	4.5 ± 0.7	7.0 ± 0.8	6.4 ± 0.7	6.2 ± 0.7
R_{SB}/r_{RL}	0.5 ± 0.1	0.5 ± 0.1	–	0.7 ± 0.1	0.6 ± 0.1	–
V_{syn} (km s^{-1})	70 ± 10	70 ± 8	–	100 ± 10	90 ± 9	–
i (°)	54 ± 17	50 ± 15	–	37 ± 14	38 ± 11	–
T_{eff} (K)	39000	36500	34000			
BC	−3.62	−3.42	−3.22			

where (a) is the total semi-major axis of the binary system, we obtain $R^A_{RL} \sin i = r^A_{RL} = 10.1\ R_\odot$ and $R^B_{RL} \sin i = r^B_{RL} = 10.3\ R_\odot$, for components A and B, respectively. Comparing these results with the Stefan–Boltzmann radii presented in Table 7 we can see that, as supposed, both components fit well inside their Roche lobes, thus building a detached system.

Now, in order to obtain some insight about the absolute masses of both stars, we could get a rough estimate for the inclination of the orbital plane of the close pair A + B. To do so, we have to derive quantitative values of the rotational velocities and to study the hypothesis of synchronous rotation in the system.

We calculated times of synchronization for the pair A + B, following the expressions given by Zahn (1977) and Tassoul (1988) obtaining $t_{syn} \approx 6.7 \times 10^4$ and $t_{syn} \approx 0.8 \times 10^4$ yr, respectively. These methods rely on different assumptions, being the only tidal forces considered in the model by Zahn (1975, 1977), while Tassoul takes into account radiative dumping as the dominant dissipative mechanism in early-type binaries. Even though, both predicted synchronization times are short enough to consider synchronic rotation as a good hypothesis for the binary system A + B.

Under this assumption, we estimate the projected rotational velocities ($V \sin i$) for components A and B using the non-LTE model atmospheres by Auer & Mihalas (1972) for He I 4471 Å, with a T_{eff} of 35 000 K and $\log g = 4$. After convolution with different rotational velocities and comparison with the observed Gaussian full width at half maximum (GFWHM) of this line in our data, we estimate projected rotational velocities $(V \sin i)_A = 57 \pm 8$ km s^{-1} and $(V \sin i)_B = 54 \pm 8$ km s^{-1}, for each component respectively. The resulting values for the estimate inclination of the orbital plane are quoted in Table 7. If those are right, the system is not likely to present eclipses. However, further photometric studies could reveal light variations associated, for example, to tidal deformations of the binary components or reflection effects, which can be expected in systems having short periods and hot luminous components.

We plotted the locations of the components A and B on the Hertzsprung–Russell (H–R) diagram in Fig. 7, together with evolutionary tracks from Serenelli & Benvenuto (private communication) for chemical composition $X = 0.70$, $Z = 0.02$. We placed on the diagram components A and B according to the different adopted distance moduli, finding bolometric luminosities that are about 50 per cent larger if we take the larger distance modulus to Trumpler 16. The lower values of the luminosities for the O7 V and O8 V stars seem to be in better agreement with those derived for other stars in binary or multiple systems in Tr 16, such as HD 93205 (Morrell

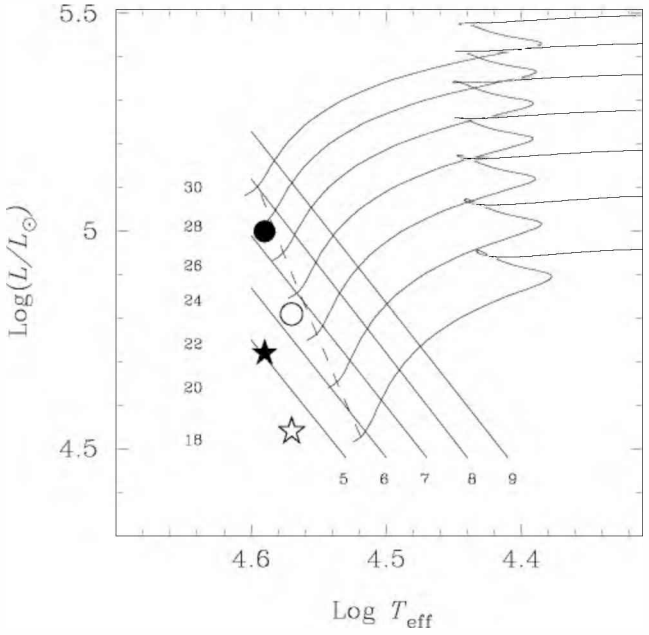

Figure 7. Position of the A (filled symbols) and B (open symbols) components on the H–R diagram. Circles and stars represent the position of the A and B components according to the distance modulus derived by Massey & Johonson (1993) and Davidson et al. (2001), respectively. Continuous lines are solar metallicity evolutionary tracks (labelled on the left-hand side with the mass of the model), and lines of constant radii (labelled at the bottom), from evolutionary models by Serenelli & Benvenuto (private communication) The dashed line represents a 0.5-Myr isochrone from the same models.

et al. 2001), Tr16-104 (Rauw et al. 2001) and Tr16-1 (Freyhammer et al. 2001), which are binaries with relatively well constrained stellar radii and luminosities. It is also interesting to point out the position of both components of the close binary A + B, to the left of the 0.5 Myr isochrone, drawn from the above-mentioned evolutionary models.

Using the estimation obtained for the orbital inclination of the A + B binary system from a lower or greater distance moduli (Table 7), and the minimum masses from our orbital solution (Table 4), we get absolute masses of $M_A \approx 21$ $M_\odot$ and $M_B \approx$ 20 $M_\odot$, or $M_A \approx 46$ $M_\odot$ and $M_B \approx 44$ $M_\odot$ respectively. If the bolometric corrections are right, we see that the bolometric luminosities and masses inferred from a lower distance to Tr 16, seem to be more realistic. They are also in better agreement with the masses suggested from a comparison with evolutionary models in Fig. 7.

These results suggest that the luminosities of main sequence O-type stars in very young clusters such as Tr 16 could be systematically smaller than usually believed, as has been previously found in a number of studies, as for example, Walborn (1995) and Walborn & Blades (1997).

6 X-RAY EMISSION

CPD −59°2636 was detected as an X-ray source by *ROSAT*. It appears in the WGACAT catalogue (White, Giommi & Angelini 1994) of Position Sensitive Proportional Counter (PSPC) sources as source 1WGA J1045.1−5944 (=2RXP J104509.1−594456) at a rate of $4.1 \pm 0.7 \times 10^{-2}$ PSPC count s^{-1}. This detection was derived from sequence rp200108n00 (observation date 1991-12-15, principal investigator W. Waldron). The source was also detected in a deep (38 ks) *ROSAT* PSPC pointing at η Carinae (rp900176, observation dates 1992 June–December, principal investigator J. Swank) at a rate of $1.18 \pm 0.07 \times 10^{-2}$ PSPC counts s^{-1}. In these PSPC pointings the source is unresolved from nearby sources, notably CPD −59°2635, CPD −59°2641 to the north and CPD −59°2629 to the south. We extracted a spectrum from the *ROSAT* sequences rp900176n00 and rp900176a01, and found we could fit the spectrum with a simple absorbed Mewe–Kaastra thin thermal emission model with $N_H = 7 \times 10^{21}$ cm^{-2} and $kT = 0.3$ KeV. The X-ray flux in the *ROSAT* band (0.2–2.4 KeV) is $f_x = 1.0 \times 10^{-13}$ erg s^{-1} cm^{-2}; the flux corrected for absorption is 1.7×10^{-12} erg s^{-1} cm^{-2}. Adopting the bolometric luminosities of Table 7 for the combined system, then the L_x/L_{bol} ratio is $\approx 1.4 \times 10^{-7}$. There is no apparent time-variability in the long PSPC exposure, though sensitivity to time-variability is poor due to contamination of the X-ray flux from CPD −59°2636 by the unresolved nearby X-ray sources.

CPD −59°2636 is also listed in the *ROSAT* Results Archive High Resolution Imager (HRI) Catalog as detection 1RXH J104512.9−594417 (sequence name 1rh900385a03.031) at $2.3 \pm 0.4 \times 10^{-3}$ HRI counts s^{-1}. This pointing occurred on 1994-07-21 and is the longest segment (40 ks) of 4 pointings centred on η Car (principal investigator J. Schmitt). Using the model which best fits the PSPC spectrum, this HRI count rate corresponds to a 0.2–2.4 keV flux $f_x = 5.0 \times 10^{-14}$ erg s^{-1} cm^{-2}, while the absorption-corrected flux is 9.8×10^{-13} erg s^{-1} cm^{-2}. These fluxes are smaller than the PSPC fluxes derived above but this is most probably due to contamination of the PSPC spectrum by neighbouring sources which are resolved from CPD −59°2636 in the HRI pointing. The HRI fluxes suggest $L_x/L_{bol} \approx 7.0 \times 10^{-8}$. Based on the L_x/L_{bol} ratios derived from the analysis of the HRI and PSPC data, there is no real evidence of any X-ray overluminosity which might be ascribed to colliding wind emission.

Because CPD −59°2636 is resolved by the HRI from most of the other strong nearby X-ray sources, we can put more sensitive limits on source variability using the HRI data than is possible with the PSPC data, to determine if the X-ray source flux is correlated with either the orbit of components A + B or component C. To generate an X-ray light curve from the HRI data, we first extracted photon events from CPD −59°2636 for all archived segments of the deep HRI η Car pointing, which, in addition to the catalogued sequence rh900385a03, include *ROSAT* sequences rh900385n00 (11 ks, observation date) and rh900385a02 (0.5 ks); another archived sequence, rh900385a01, had an accepted exposure of 0 ks and was not included for analysis. The combined *ROSAT* HRI image (50 ks effective exposure) is shown in Fig. 8. In addition to the rh900385 observations, CPD −59°2636 was also detected in another long (47 ks) HRI pointing at η Car, sequence identification rh200331n00. Prior to extracting light curves we examined the pulse-height distribution of the HRI emission for CPD −59°2636 in order to determine the importance of ultraviolet (UV) contamination produced by the HRI UV light leak. The HRI pulse height distribution peaks near HRI channel 6, while UV photons have a pulse height distribution peaking at HRI channels <3; thus UV contamination is rather minimal for CPD −59°2636. We then extracted light curves from the rh900385 sequences and from rh200331n00 from a ∼20-arcsec radius region centred on CPD −59°2636, using a neighbouring source-free region to estimate background, using a time bin size of 5 ks. The resulting light curves (Fig. 9) have rather good phase coverage, but show no significant variability correlated with the orbital phase of either component C or components A + B. Given the lack of any X-ray variability and the rather modest X-ray luminosity of CPD −59°2636 in the *ROSAT* pointings, there is no strong evidence of X-ray emission from wind–wind collisions in this source. This is

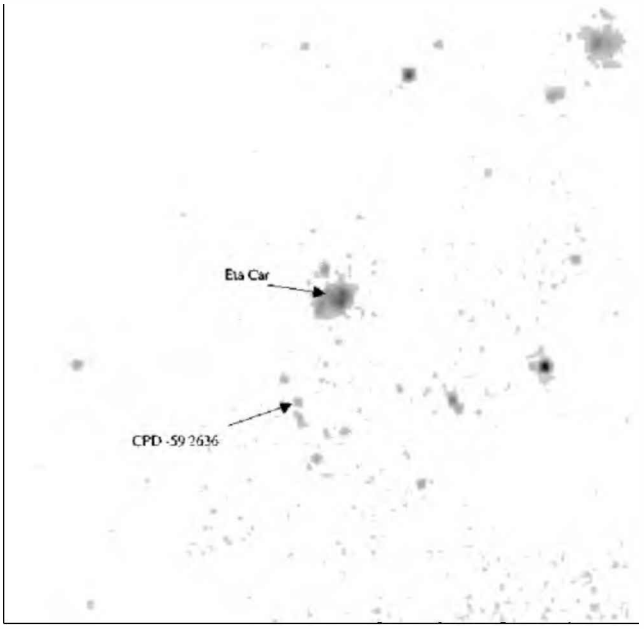

Figure 8. 50-ks *ROSAT* HRI image of the Carina Nebula. The location of CPD −59°2636 is marked.

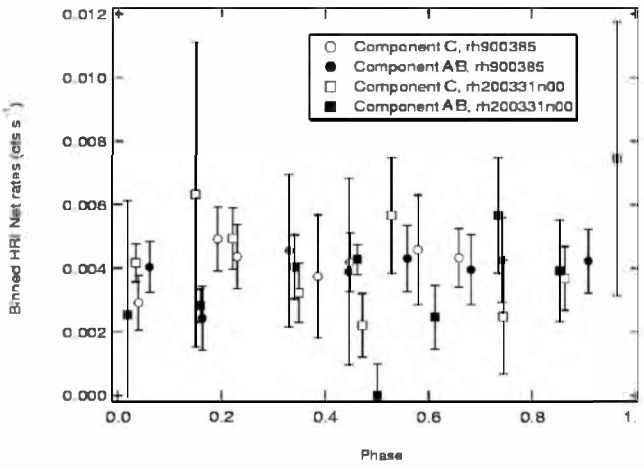

Figure 9. Light curves extracted from *ROSAT* HRI pointings at CPD −59°2636. The observing times have been phased using the periods of components A + B and of component C, using an arbitrary epoch.

somewhat surprising given the presence of at least three O-type stars in this system. It might be that some or most of the colliding wind X-ray emission is generated at energies beyond the *ROSAT* passband, or alternatively, perhaps the emission is suppressed by circumstellar absorption or radiative braking (Gayley, Owocki & Cranmer 1997).

7 CONCLUSIONS

We have demonstrated that CPD −59°2636 is a new special O-type multiple system composed of two binary stars. Three sets of absorption lines are observed in the high-resolution spectra, which we labelled as components A, B and C, with spectral types O7 V, O8 V and O9 V, respectively. Radial velocity measurements and analysis showed that component C is a single-lined binary with a 5.034-d period, and components A and B form a double-lined binary system with a 3.6284-d period.

Adopting for Trumpler 16 the distance modulus obtained by Davidson et al. (2001) (i.e. 11.76 mag), the place of components A and B on a log $T_{\rm eff}$ versus log $L/L_{\odot}$ diagram corresponds to evolutionary tracks of ~22 and 18 $M_{\odot}$, in agreement with the masses estimated using the parameters of the system and an inclination ~52° (derived from the observed linewidths under the assumption of synchronous rotation). Moreover, both binary components seem to be well within their Roche lobes, and lie to the left of the 0.5-Myr isochrone on the same diagram.

Although, because of the probable low value of the inclination, the SB2 binary system is not likely to present eclipses, future photometric studies could reveal light variations due to tidal deformation or reflection effects.

CPD −59°2636 was detected by *ROSAT* as an X-ray source with the PSPC and HRI cameras. No real evidence of overluminosity is observed in the X-ray data, although it could be expected in a system having three O-type stars. This might suggest heavy circumstellar absorption or a radiative braking mechanism acting in this multiple system. X-ray light variations were not detected in the PSPC and HRI observations.

ACKNOWLEDGMENTS

We thank the director and staff of CASLEO for technical support and kind hospitality during the observing runs. We acknowledge use at CASLEO of the CCD and data acquisition system provided through US NSF grant AST-90-15827 to R. M. Rich. We thank Eric Gosset who obtained one of the FEROS spectra in May 1999. We are grateful to Aldo Serenelli and Omar Benvenuto for the use of their massive stars evolutionary models and useful discussions. We thank Nolan Walborn for many very useful comments and improving the English of an earlier version of this work, and our referee, Ian D. Howarth, for helpful suggestions. This research has made use of NASA's Astrophysics Data System Abstract Service. This research has made use of data obtained from the High Energy Astrophysics Science Archive Research Centre (HEASARC), provided by NASA's Goddard Space Flight Centre. Useful discussions with R. Barbá are very much appreciated.

REFERENCES

Albacete Colombo J. F., Morrell N., Niemela V., Corcoran M., 2001, MNRAS, 326, 78
Auer L. H., Mihalas D., 1972, ApJS, 24, 193
Bagnuolo W. G., Gies, D. R., Riddle R., Penny L. R., 1999, ApJ, 527, 353
Benvenuto O., Serenelli A., Althaus l., Morrell N., Barbá R., 2002, MNRAS, 330, 435
Bertiau F. C., Grobben J., 1969, Ric. Astronom. Sp. Vaticana, 8, 1
Chlebowski T., Garmany C. D., 1991, AJ, 368, 241
Cincotta P., Mendez M., Nuñez J., 1995, ApJ, 449, 231
Conti P. S., 1973, ApJ, 179, 181
Conti P. S., Alschuler W. R., 1971, ApJ, 170, 325
Corcoran et al., 1999, in van der Hucht K. A., Koenigsberger G., Eenens P. R. J., eds, Proc. IAU Symp. 193, Wolf-Rayet Phenomena in Massive Stars and Starburst Galaxies. Astron. Soc. Pac., Chelsea, p. 772
Davidson K., Smith N., Gull R. T., Ishibashi K., Hillier D. J., 2001, AJ, 121, 1569
Eggleton P. P., 1983, ApJ, 268, 368
Eggleton P., Kiseleva L., 1995, ApJ, 455, 640
Feinstein A., Marraco H. G., Muzzio J. C., 1973, A&AS, 12, 331
Freyhammer L., Clausen J. V., Arentoft T., Sterken C., 2001, MNRAS, 284, 265

Gayley K. G., 2001, in Moffat A. F. J., St.-Louis N., eds, ASP Conf. Ser. Vol. 260, Interacting Winds from Massive Stars. Astron. Soc. Pac., San Francisco, p. 583
Gayley K. G., Owocki S. P., Cranmer S. R., 1997, ApJ, 475, 786
Heck A., Manfroid J., Mersch G., 1985, A&AS, 59, 63
Howarth I. D., Prinja R. K., 1989, ApJS, 69, 527
Kaufer A., Stahl O., Tubbesing S., 1999, The Messenger, 95, 8
Kerton C. R., Ballantyne D. R., Martin P. G., 1999, AJ, 117, 2493
Lafler J., Kinman T. D., 1965, ApJS, 11, 199
Levato H., Malaroda S., 1982, PASP, 94, 807
Levato H., Malaroda S., Morrell N., García B., Hernández C., 1991, ApJS, 75, 869
Lucy L. B., Sweeney M. A., 1971, AJ, 76, 544
Massey P., Johnson J., 1993, AJ, 105, 980
Mathys P., 1988, A&AS, 76, 427
Morrell N. et al., 2001, MNRAS, 326, 85
Paczynski B., 1971, Ann. Rev. Astron. Astrophys., 9, 183
Petrie R. M., 1940, Publ. Dom. Astroph. Obs. Victoria, 7, 205
Rauw G., Sana H., Antokhin I. I., Morrell N. I., Niemela V. S., Albacete Colombo J. F., Gosset E., Vreux J. M., 2001, MNRAS, 336, 1149
Tassoul J.-L., 1988, ApJ, 324, 71
Turatto M., Tighe R., Castillo R., 1997, ESO Technical Report, E15-TRE-ESO-22201-00001
Walborn N., 1982a, ApJS, 48, 145
Walborn N., 1982b, AJ, 87, 1300
Walborn N., 1995, Rev. Mex. Astron. Astrofis. Ser. Conf., 2, 51
Walborn N., Blades J. C., 1997, ApJS, 112, 457
Walborn N., Fitzpatrick E., 1990, PASP, 102, 379
White N. E., Giommi P., Angelini L., 1994, IAUC, 6100, 1
Zahn J.-P., 1975, A&A, 41, 329
Zahn J.-P., 1977, A&A, 57, 383

This paper has been typeset from a TEX/LATEX file prepared by the author.